CRS-attribute-based residual static correction

I. Koglin and E. Ewig

email: *Ingo.Koglin@gpi.uni-karlsruhe.de*
keywords: *residual static correction, CRS moveout*

ABSTRACT

Residual static corrections are of great interest for onshore datasets. There, they are used to eliminate the influence on reflection traveltimes of the weathering layer and/or any errors introduced by redatuming methods. Thus, the results of stacking methods applied after residual static corrections should show an improved signal-to-noise ratio. We considered to make use of the Common-Reflection-Surface stack which provides additional information about the subsurface by means of kinematic wavefield attributes that define a stacking surface within a spatial aperture rather than within the common-midpoint gathers, only. Thus, these attributes serve as a basis for a moveout correction which is mandatory for the determination of residual statics. The first results of a small and not too complex real data example show that our new approach is able to estimate residual statics.

INTRODUCTION

Onshore real data acquisition is often influenced by topography and irregularities in the near surface, e. g., the weathering layer. The topographic effect on the reflection times is significantly reduced by applying so-called field static corrections. However, the effects of rapid changes in elevation and in near-surface velocity or thickness of the weathering layer still remain as reflection time distortions. To eliminate these remains which the field static correction did not compensate, the residual static correction assigns every shot and every receiver an additional static time shift. The time shifts of residual static corrections aim at enhancing the continuity of the reflection events and at improving the signal-to-noise (S/N) ratio after stacking.

The 2D zero-offset (ZO) Common-Reflection-Surface (CRS) stack method has shown its abilities to improve the S/N ratio under the assumption of a horizontal plane measurement surface (see Trappe et al., 2001). Zhang (2003) has introduced the topography into the CRS stack method. This can be seen as a more sophisticated kind of field static correction. As stacking methods in general, the 2D ZO CRS stack method does not directly account for residual static corrections. Similar to the conventional common-midpoint (CMP) based methods, a new alternative approach of residual static correction based on the CRS attributes is presented in the following.

BASICS OF STATIC CORRECTIONS

The main assumption for applying static corrections is surface consistency. This implies that the waves propagate nearly vertical through the uppermost layer and, hence, independent from the raypaths in the deeper layers. Thus, the time shifts become properties of the source or receiver locations, only. Furthermore, the reflection time distortions do not depend on the traveltime of different reflection events, i. e., are reflection time independent and, therefore, these time shifts are called static corrections. Another assumption is that the uppermost layer, i. e., the weathering layer, has the same influence on the shape of the wavelet of all emerging reflection events. The latter assumption is due to the fact that we do not account for phase shifts on the wavelet at the moment.

Under these assumptions, static corrections can be divided into two parts:

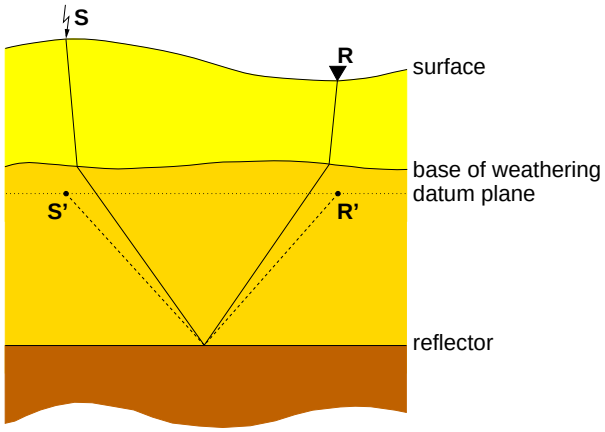

Figure 1: Raypath through a low velocity layer. Redatuming achieved by field static correction substitutes the actual surface by a reference datum plane beneath the low velocity layer, i. e., source S and receiver R are moved to S' and R' on the reference datum plane, respectively.

- The field static correction, which is a kind of redatuming, introduces a "reference datum plane" as substitute for the actual measurement surface and is mostly located beneath the weathering layer (see Figure 1). For further explanations, please refer to Marsden (1993).
- The residual static correction is used to eliminate small variations of reflection traveltimes caused by the weathering layer. Additionally, errors from redatuming by field static correction or other methods can be removed. Even though, residual static correction can be also applied without any preceeding static correction to enhance the imaging quality.

Conventional residual static correction methods

To achieve surface consistency, residual static correction techniques have to provide exactly one time shift for every source or receiver location, respectively. The first step of most of the conventional residual static correction techniques is to apply an approximate normal moveout (NMO) correction. Then, the reflection events in each CMP gather are considered to be misaligned due to a source static, a receiver static, a residual moveout, and additional terms depending on the used method. The calculated time shifts t_{ij} of each trace consist of the following terms

$$t_{ij} = t_{r_i} + t_{s_j} + M_k X_{ij}^2 + \ldots \quad \text{with} \quad k = \frac{i+j}{2} \tag{1}$$

where t_{r_i} is the receiver static of the i-th receiver location and t_{s_j} is the source static for the j-th source location. M_k is the residual moveout at the k-th CMP gather and $X_{ij} = r_i - s_j$ is the source to receiver distance or simply the offset (see Taner et al., 1974; Wiggins et al., 1976; Cox, 1974) with the source location s_j and the receiver location r_i. Figure 2 shows an example of the improvements of the stacking result due to residual static correction. Figure 2(a) shows a reflection event after NMO correction distorted by residual statics. Stacking these traces without any corrections results in a deformed wavelet (see Figure 2(b)), while the stack with residual static correction clearly shows a well preserved wavelet with larger amplitudes due to the coherent stack (see Figure 2(c)).

From this point on, a lot of different conventional methods exist to determine t_{ij} or t_{r_i} and t_{s_j}, respectively. One method, e. g., is to cross correlate all traces of each CMP gather with their corresponding CMP stacked trace which is used as pilot trace for this CMP gather. The window for the correlation has to be selected to cover more than one dominant primary event (time invariance) and at reasonably large traveltimes (surface consistency). Thus, a system of equations of t_{ij} is given by one equation for each trace of the whole dataset. This large system of linear equations is overdetermined, i. e., there are more equations than

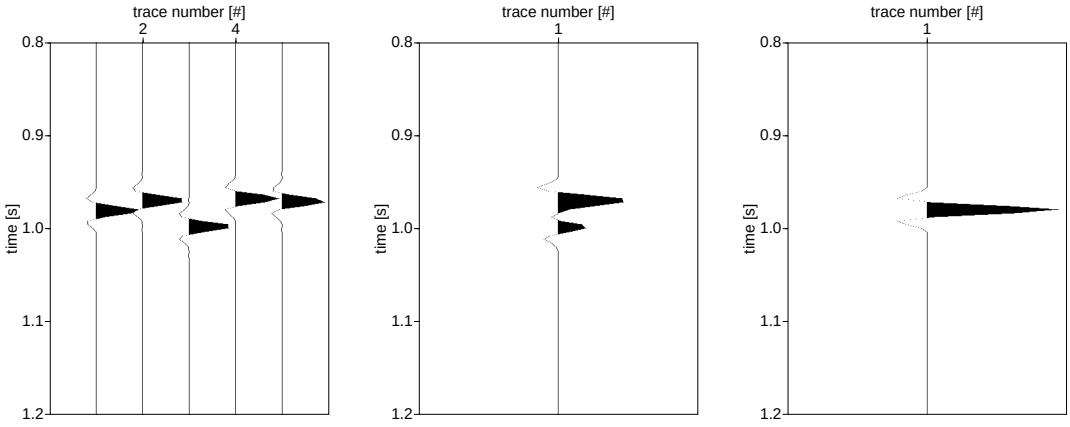

(a) synthetic gather **(b)** stacked 'as is' **(c)** with residual static correction

Figure 2: Example of the enhancement due to residual static correction after an approximate NMO correction.

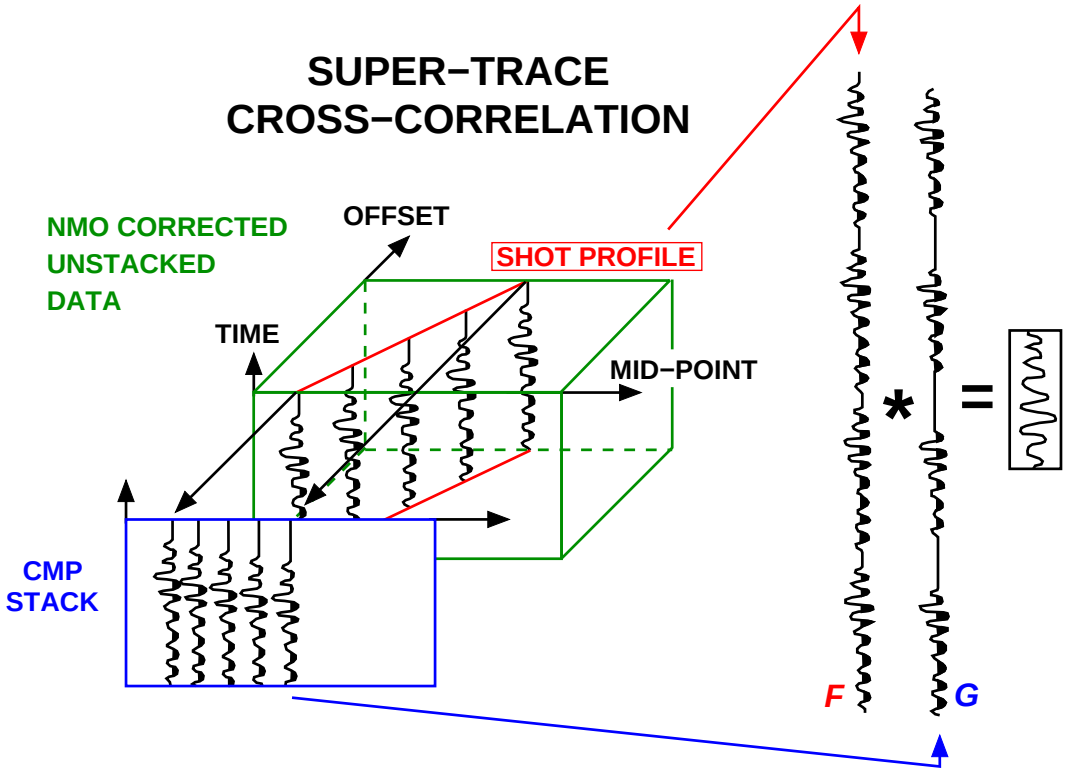

Figure 3: Example of super-traces for one moveout corrected shot gather. Super-trace F and super-trace G are cross correlated to determine the corresponding source static. Figure taken from Ronen and Claerbout (1985).

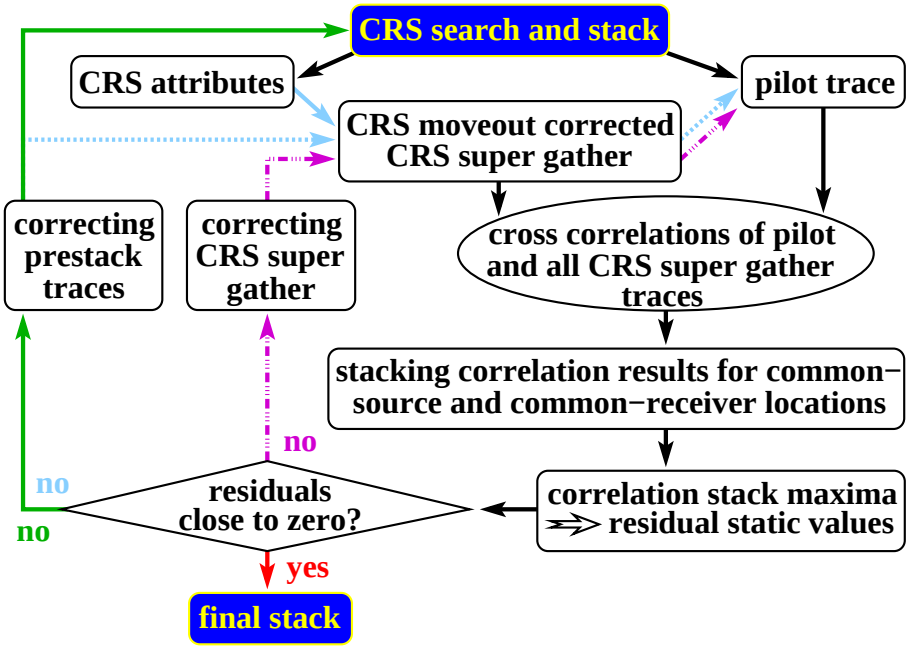

Figure 4: Flowchart for the iterative residual static correction by means of CRS attributes. Three alternatives are available for the second and further iterations: the CRS search for the attributes can be optionally performed again (solid green arrows). If not (see dashed and solid blue arrows), the pilot trace has to be recalculated from the CRS moveout corrected CRS super gather to take advantage of the enhancements of the previous iterations. A third option (dash-dotted purple arrows) can be used to directly correct the previously calculated CRS super gather with the obtained residual static values.

unknowns, and underconstrained, i. e., there are more unknowns than independent equations. The solution is generally obtained by least-square techniques.

Ronen and Claerbout (1985) introduced another technique based on cross correlation, the stack power maximization method. Here, the cross correlation is performed between so-called super-traces. A super-trace built from all the traces of the shot profile in sequence (trace F in Figure 3) is cross correlated with another super-trace analogously built of all traces in the relevant part of the stack without the contribution of that shot (trace G in Figure 3). The source static of this shot is the time associated with the global maximum of the cross correlation result. This procedure is repeated for every shot and receiver profile, respectively. The resulting time shifts maximize the sum of squared amplitudes of the final stack, i. e., the stack power.

NEW APPROACH BY MEANS OF CRS ATTRIBUTES

In addition to the simulated ZO section, the CRS stack method provides three further sections with CRS attributes. These attributes (α, R_{NIP}, R_{N}) are parameters of the second-order stacking surface given by

$$t_{hyp}^2(x,h) = \left[t_0 + \frac{2}{v_0}(x-x_0)\sin\alpha\right]^2 + \frac{2}{v_0}t_0\cos^2\alpha\left[\frac{(x-x_0)^2}{R_{\mathrm{N}}} + \frac{h^2}{R_{\mathrm{NIP}}}\right], \qquad (2)$$

with the ZO traveltime t_0, the near-surface velocity v_0, the emergence angle α of the ZO ray, the radius of curvature of the NIP wavefront R_{NIP} measured at x_0, and the radius of curvature of the normal wavefront R_{N} also measured at x_0 (see, e. g., Mann et al., 1999, for these definitions). This stacking surface from the CRS stack method improves the S/N ratio more than, e. g., the NMO/DMO/stack method due to the larger stacking surface (see Mann, 2002; Trappe et al., 2001).

Our new approach is also based on cross correlations and is similar to the technique of Ronen and Claerbout (1985). Figure 4 shows the principal steps of our method. The first step is to perform at least the

initial 2D ZO CRS stack to obtain the CRS attribute sections and the simulated ZO section. Each trace of the simulated ZO section serves as a pilot trace for the necessary cross correlations. Additionally, the optimized 2D ZO CRS stack can also be used for the subsequent steps. However, this requires more processing time due to a local optimization of the attributes. The initial CRS stack differs from the optimized one by the strategy to obtain the attributes. The attributes of the initial search serve as starting values for the optimized search. Irrespectively how the attributes are obtained, the CRS moveout correction is then realized with the previously obtained CRS attributes.

CRS moveout correction

To correct for the CRS moveout, the dependency on the half-offset h and the midpoint x in equation (2) has to be eliminated. Therefore, the CRS attributes of every time sample within the simulated ZO section are required. These attributes are provided by the initial or optimized search of the CRS stack method. With the knowledge of these attributes, the Common-Reflection-Surface can be transformed into a horizontal plane at time t_0 by subtracting the moveout given by

$$t_{moveout}(x,h) = t_{hyp}(x,h) - t_0\,, \tag{3}$$

where t_0 is given by the considered time sample of the simulated ZO section.

This correction is performed for all t_0 given by each simulated ZO trace of the CRS stack. The result for one ZO trace is called CRS moveout-corrected CRS super gather and contains all CRS moveout corrected prestack traces which lie inside the corresponding spatial CRS aperture. Thus, the prestack traces are multiply contained in the differentCRS super gathers with different moveout corrections in each super gather.

Cross correlation

The cross correlations are performed between every single moveout corrected trace of each CRS super gather and the corresponding trace of the simulated ZO section, i. e., the pilot trace. These correlations can also be weighted with the coherence values provided by the CRS stack to account for the reliability of every single sample. Afterwards, all correlation results that belong to the same source or receiver location are summed up. These cross correlation stacks are similar to cross correlating super-traces as proposed by Ronen and Claerbout (1985).

The main difference to CMP-gather-based methods is that the correlation of the super-traces accounts for the subsurface structure because super-trace G of Figure 3 is a sequence of neighboring stacked traces and not of one stacked trace repeated multiple times. Super-trace F consists of all traces belonging to the same source or receiver location, respectively. The CRS stack accounts for the subsurface structure by means of the CRS attribute R_{N} which enters into the CRS moveout correction. R_{N} is the radius of curvature of the normal wave measured at the surface and can be associated with an hypothetical exploding reflector experiment.

Finally, the residual static value is given by the time associated with the global maximum of the summed correlation results. In future, local extrema may be additionally considered to estimate the reliability of the global maximum. In case of phase shifts, the global minimum may represent the searched for residual static value. The decision whether there are phase shifts or not also depends on the shape of the correlation result close to the global minimum and has to be performed for every trace before the correlation stack. This will be also implemented in future.

Problems might occur at the boundary of the dataset because there only few correlation results will contribute to source or receiver locations. Therefore, we implemented a threshold for the maximum correlation shift, i. e., a maximum residual static time shift. This threshold also reduces the likelyhood of cycle skips.

Iteration

Once the residual static values are obtained from the cross correlation results, the prestack traces are time shifted with the corresponding total time shifts. The total time shift is simply the sum of the corresponding

source and receiver static values of each prestack trace. If the CRS stack of these corrected prestack traces is not yet satisfactory, the entire procedure can be started again in two different ways with the previously corrected prestack traces or, in an alternative way, with the previously corrected CRS super gathers. The first possibility is to perform the CRS search and all other steps (see solid green arrows in Figure 4). The second possibility omits the CRS search for the attributes (see dashed blue arrows in Figure 4). As the CRS search for the attributes is the most time consuming step of our method, it is attractive to omit this step. However, it might be dangerous to rely on the CRS attributes: if the time shifts between neighboring traces are too large, the CRS stack probably fails to detect actually contiguous events and the corresponding attributes. The third possibility is to use the obtained residual static values to directly correct the traces of the CRS super gathers. However, this possibility is not surface-consistent as the static time shifts are applied to moveout corrected traces. Thus, the corresponding prestack traces are no longer shifted by a static time, every time sample of one trace has to be shifted by different times. As one prestack trace is multiply contained in the CRS super gathers but with different moveout corrections, the time shifts for each sample also depend on the actual midpoint and its associated moveout correction. Some results for the second and third possibility as well as combinations of all three possibilities can be found in Ewig (2003).

REAL DATA EXAMPLE

A CMP-based residual static correction method was applied to a not too complex real dataset by Kirchheimer (1990). There, the original dataset was perturbed by synthetic receiver statics which afterwards had to be estimated by the chosen residual static method. We were provided with this real dataset after conventional residual static methods had been applied. Thus, we tested our new approach with a small subset of 100 CMP gathers of this real dataset with a CMP fold of ≈ 30 and a sampling rate of 2 ms. This part contains only slightly dipping reflectors. The vertical bands of small amplitudes and gaps mainly at small traveltimes are due to the aquisition geometry and the relatively small number of traces. Figure 5 a) shows the result of the optimized CRS stack applied without our residual static correction method.

We started with applying our new approach directly to the provided dataset to see whether there remained some residual statics in the provided dataset (see Figure 5 a)). We performed two iterations with a new CRS attribute search in each step. The result is shown in Figure 5 b). The estimated residual statics of the second iteration were mostly zero and therefore we tested only the residual static estimation for the third iteration. The source residual statics of the third iteration were zero for all locations and the receiver residual statics were zero except for a few locations with -1 ms. Therefore, we expected only slight changes from the second to the third iteration and omitted the CRS stack. Figure 7 shows the obtained residual statics after the second iteration for source and receiver locations.

To further test our method with this dataset, we added random but surface consistent residual time shifts for all source (dashed red line in Figure 8) and receiver (dashed blue line in Figure 8) locations to the provided dataset. Both, the added source and receiver time shifts are between -10 and $+10$ ms with zero mean. Thus, the total time shifts are between -20 and $+20$ ms. Figure 6 a) shows the optimized CRS stack result of the artifically distorted prestack traces with the same amplitude range as in Figures 5. The synthetic residual time shifts almost completely destroyed the stacking result. Now, we applied again our new approach to this dataset. The obtained residual statics of the fifth iteration step are zero with a few variations of ± 1 ms. The result of the optimized CRS stack after the fifth iteration is shown in Figure 6 b). In comparison to the CRS stack of the provided dataset (Figure 5 a)), we can say that we reproduced almost perfectly the provided dataset.

Figures 8 a) and 8 b) show the summed results of the five iterations (green solid lines) for the residual source (red dashed line) and receiver (blue dashed line) statics, respectively. The fact that the obtained residual statics do not perfectly match the synthetic added ones is due to the correlation stacking and the dataset itself. On the one hand, during the cross correlation stacking for, e. g., one source location, it is assumed that the residual statics of the receiver locations within the CS gather diminish and vice versa. On the other hand, our method has found some minor residual statics in the provided dataset which were not corrected before we added the synthetic statics.

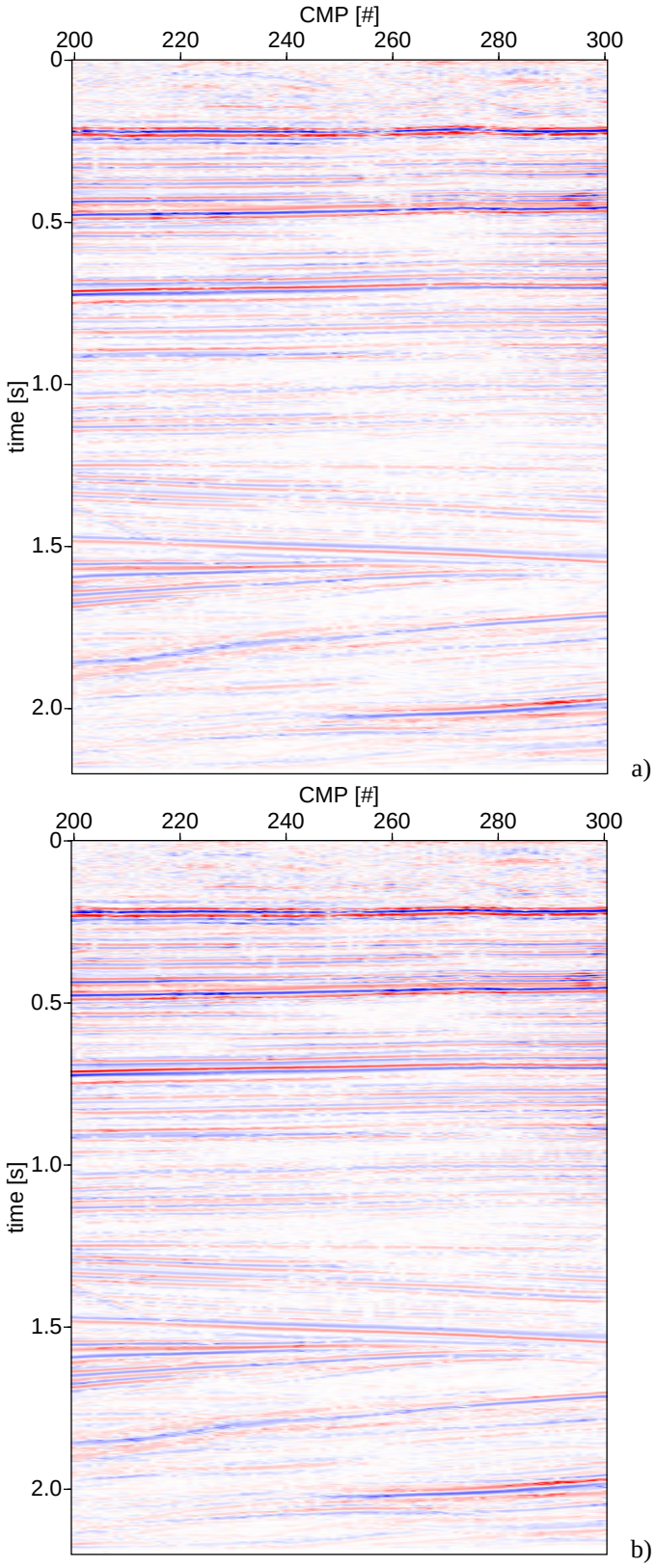

Figure 5: Simulated ZO section of the optimized CRS stack a) from the provided dataset and b) after two iterations of our residual static correction method with a new CRS attribute search in each step.

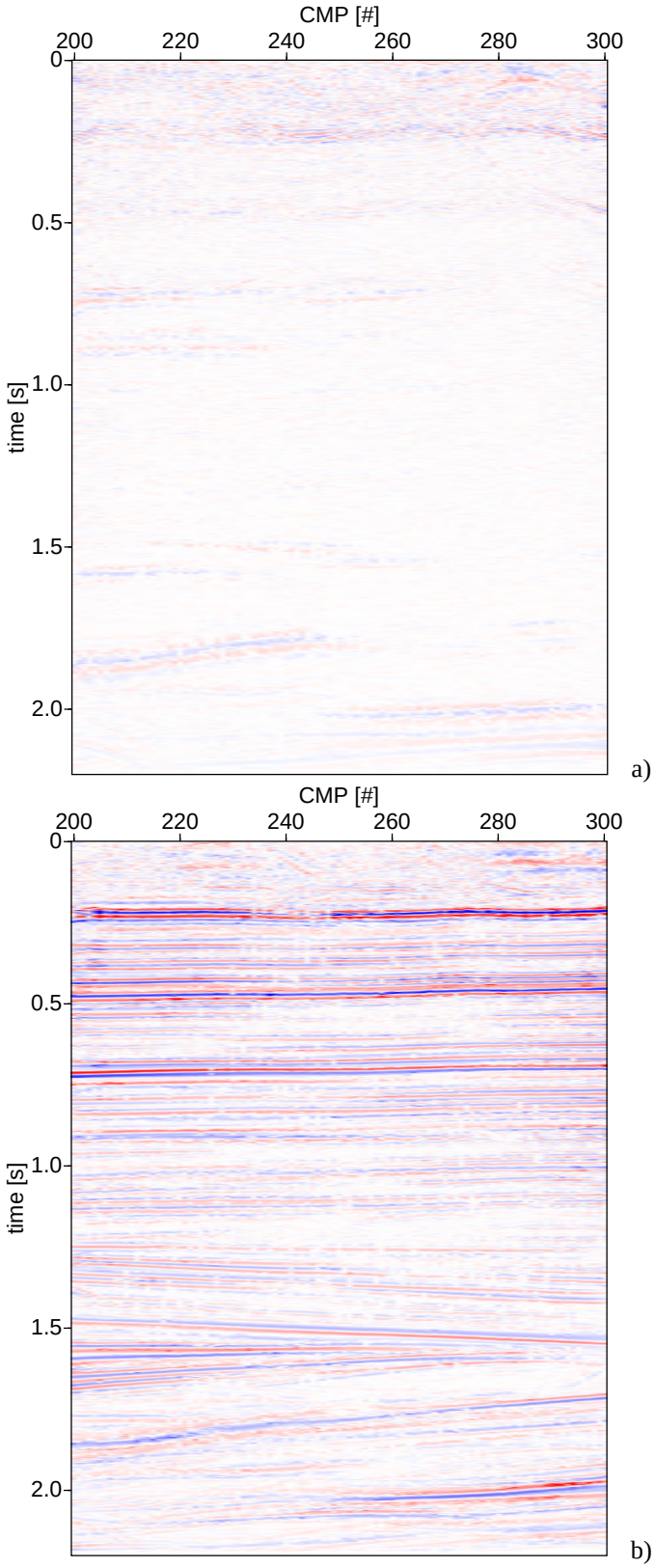

Figure 6: Simulated ZO section of the optimized CRS stack a) after random but surface consistent residual statics added to the prestack traces and b) after five iterations of our residual static correction method with a new CRS attribute search in each step.

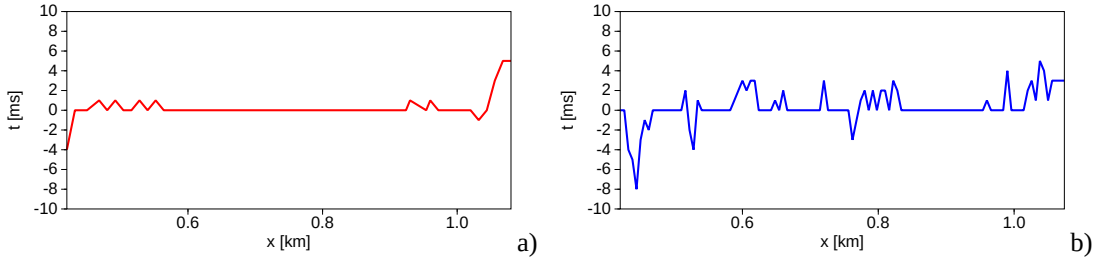

Figure 7: Obtained residual statics after two iterations applied to the provided dataset. a) source residual statics and b) receiver residual statics.

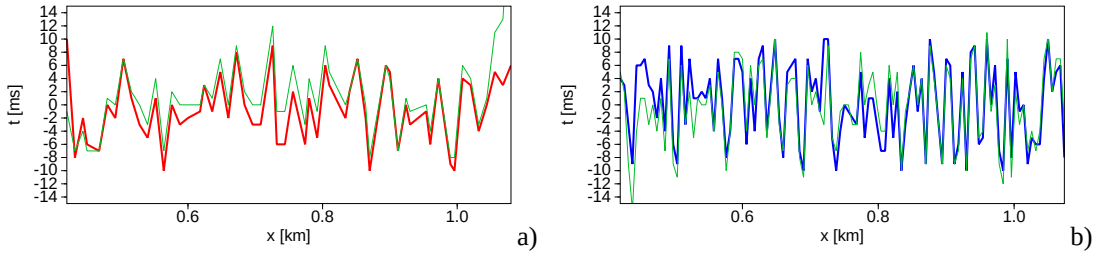

Figure 8: Statics: the obtained residual statics after the fifth iteration are shown as green lines. a) random added residual source time shifts as red dotted line and b) random added residual receiver time shifts as blue dotted line.

CONCLUSIONS

Residual static correction methods are, in general, based on cross correlations. We showed that the CRS stack method can help to derive the residual statics. The advantages of the CRS stack method, i. e., the improved S/N ratio and the additional information about the subsurface by the CRS attributes compared to, e. g., the NMO/DMO/stack, is integrated into our new approach. The CRS stack method fits entire surfaces to reflection events which is essential for a moveout correction within a spatial aperture. Also, the traces of the simulated ZO section are better suited as pilot traces than simply CMP stacked traces because of the large spatial aperture. Our new approach combines the conventional methods (cross correlation, picking maxima) with the improvements of the CRS stack. Here, the large spatial aperture of the CRS stack takes far more traces into account than just correlating within CMP gathers. Furthermore, the coherence of the CRS stack serves as a reliability weight for the traces during the cross correlation.

As displayed in Figure 6 b), the results of the first test with a small subset of a real dataset showed that this new approach is able to enhance the simulated ZO section of datasets distorted by residual statics. Thus, more effort will be put in the determination of the residual static values in future. Despite of simply picking the global maximum of the summed cross correlation results, also the neighboring extrema can be accounted for to evaluate the reliability and to detect possible phase shifts.

PUBLICATIONS

Detailed results were published by Ewig (2003).

ACKNOWLEDGMENTS

This work was kindly supported by the sponsors of the *Wave Inversion Technology (WIT) Consortium*, Karlsruhe, Germany. Additional thanks go to Dr. Franz Kirchheimer for his ideas and suggestions and to Dr. Jürgen Mann for his help in implementing the new approach into the CRS code.

REFERENCES

Cox, M. (1974). *Static Correction for Seismic Reflection Surveys*. Society of Exploration Geophysicists.

Ewig, E. (2003). Theory and application of residual static correction by means of CRS attributes. Master's thesis, Universität Karlsruhe, Germany.

Kirchheimer, F. (1990). Residual statics by CDP-localized stack optimization. *Geophys. Prosp.*, 38:577 – 606.

Mann, J. (2002). *Extensions and Applications of the Common-Reflection-Surface Stack Method*. Logos Verlag, Berlin.

Mann, J., Jäger, R., Müller, T., Höcht, G., and Hubral, P. (1999). Common-reflection-surface stack – a real data example. *J. Appl. Geoph.*, 42(3,4):301–318.

Marsden, D. (1993). Static corrections—a review. *The Leading Edge*, 12(1):43 – 49.

Ronen, J. and Claerbout, J. F. (1985). Surface-consistent residual statics estimation by stack-power maximization. *Geophysics*, 50(12):2759 – 2767.

Taner, M. T., Koehler, F., and Alhilali, K. A. (1974). Estimation and correction of near-surface anomalies. *Geophysics*, 39(4):441 – 463.

Trappe, H., Gierse, G., and Pruessmann, J. (2001). Case studies show potential of Common Reflection Surface stack – structural resolution in the time domain beyond the conventional NMO/DMO stack. *First Break*, 19(11):625 – 633.

Wiggins, R. A., Larner, K. L., and Wisecup, R. D. (1976). Residual static analysis as a general linear inverse problem. *Geophysics*, 41(5):922 – 938.

Zhang, Y. (2003). *Common-Reflection-Surface Stack and the Handling of Top Surface Topography*. Logos Verlag, Berlin.